


A DISTRIBUTION-AWARE FLOW-MATCHING FOR GENERATING UNSTRUCTURED DATA FOR FEW-SHOT REINFORCEMENT LEARNING

A PREPRINT

 **Mohammad Pivezhandi***
Department of Computer Science
Wayne State University
Detroit, MI 48202
pivezhandi@wayne.edu

 **Abusayeed Saifullah†**
Department of Computer Science
Wayne State University
Detroit, MI 48202
saifullah@wayne.edu

September 24, 2024

ABSTRACT

Generating realistic and diverse unstructured data is a significant challenge in reinforcement learning (RL), particularly in few-shot learning scenarios where data is scarce. Traditional RL methods often rely on extensive datasets or simulations, which are costly and time-consuming. In this paper, we introduce a distribution-aware flow matching, designed to generate synthetic unstructured data tailored specifically for an application of few-shot RL called Dynamic Voltage and Frequency Scaling (DVFS) on embedded processors. This method leverages the sample efficiency of flow matching and incorporates statistical learning techniques such as bootstrapping to improve its generalization and robustness of the latent space. Additionally, we apply feature weighting through Random Forests to prioritize critical data aspects, thereby improving the precision of the generated synthetic data. This approach not only mitigates the challenges of overfitting and data correlation in unstructured data in traditional Model-Based RL but also aligns with the Law of Large Numbers, ensuring convergence to true empirical values and optimal policy as the number of samples increases. Through extensive experimentation on an application of DVFS for low energy processing, we demonstrate that our method provides a stable convergence based on max Q-value while enhancing frame rate by 30% in the very beginning first timestamps, making this RL model efficient in resource-constrained environments.

Keywords Dynamic Voltage and Frequency Scaling, Few-shot learning, Laws of Large Numbers, Model-Based Reinforcement Learning

1 Introduction

The rapid advancements in large-scale generative models have transformed how we approach data generation, particularly in structured domains like computer vision to generate image and video. Techniques such as diffusion models Ramesh et al. [2022], Saharia et al. [2022], Croitoru et al. [2023] have shown remarkable success in generating high-quality data, prompting a surge of interest in understanding and leveraging the underlying latent spaces for various applications. However, the challenge of generating realistic and diverse unstructured data that lacks a predefined format or organization remains largely underexplored. This challenge becomes even more pronounced in the context of few-shot learning, where models must learn to generalize from a minimal number of examples. In this case both a sample efficient learning models and a low-cost samples to train these models do matter. Addressing this is crucial for advancing online reinforcement learning (RL) in environments characterized by unstructured data, such as sensor

*Wayne State University. Email: pivezhandi@wayne.edu

†Wayne State University. Email: saifullah@wayne.edu

readings in DVFS. DVFS is a commonly used power-management technique where the clock frequency of a processor is decreased to allow a corresponding reduction in the supply voltage. This reduces power consumption, which leads to reduction in the energy required for a computation.

In this paper, we introduce a novel approach called distribution-aware flow matching, designed to generate synthetic unstructured data that is specifically tailored for few-shot RL. Unlike traditional data generation techniques that often require extensive datasets or rely on environment simulations, our approach focuses on creating diverse and realistic data samples from limited real-world trajectories. We achieve this by leveraging flow matching, a powerful method that offers simulation-free training of continuous normalizing flows (CNFs), thereby improving both the efficiency and quality of the generated data compared to standard diffusion models Lipman et al. [2022]. By integrating statistical techniques such as bootstrapping Efron [1992] into the flow matching process, we enhance the latent space representation, enabling the model to generalize better across various scenarios. Furthermore, we employ feature selection methods, such as Random Forests, to prioritize the most critical aspects of the data, ensuring that the generated synthetic data captures the essential characteristics needed for effective learning. This approach not only improves the robustness and diversity of the synthetic data but also aligns with the principles of the Law of Large Numbers (LLN) Hastie et al. [2009], ensuring that empirical estimates converge to their true values as more samples are generated. This principle also ensures the regret coefficient as the difference between the optimal RL model decision and the taken decision is minimized Foster and Rakhlin [2023].

Our approach addresses the limitations of conventional model-based RL methods, which often struggle with issues like overfitting and feature correlation when applied to unstructured data. We demonstrate that feature correlation increases when generating synthetic data using these conventional methods, as their predictions rely heavily on real data. This correlation reduces the synthetic data’s resemblance to real scenarios and diminishes the RL agent’s robustness in handling edge cases. By generating synthetic data that closely mirrors real-world scenarios, distribution-aware flow matching significantly enhances the adaptability and performance of RL models in few-shot learning settings. This is particularly valuable in dynamic and resource-constrained environments, where real-time adaptability is critical. Through extensive experimentation and evaluation, we demonstrate that our method not only increases sample efficiency but also provides a robust framework for generating unstructured data that supports few-shot reinforcement learning. This method is integrated into Dynamic voltage and frequency scaling (DVFS) technology to improve the performance and reliability of embedded systems. An energy-efficient DVFS strategy can reduce power consumption by 75% without altering the user experience Ratković et al. [2015]. This method also has broader applications in fields such as autonomous systems, robotics, and complex decision-making processes, where the ability to quickly adapt to new situations with minimal data is essential.

2 Preliminaries

DVFS Application. DVFS is a technology used to adjust the voltage and frequency of processor cores to conserve power and control temperature while maintaining operational performance. The states in this context are interrelated continuous unstructured data, including frames per second (*fps*), power consumption (ρ), frequency (f), and temperature (θ). For any processor comprising CPUs and GPUs, the total power consumption is given by $\rho = \rho_d + \rho_s$, where ρ_d represents dynamic power consumption and ρ_s represents static power consumption. Dynamic power consumption ρ_d is proportional to f^η , where f is the frequency and $\eta > 2$ is a technology-dependent constant Xie et al. [2017]. Static power consumption ρ_s is proportional to the core temperature θ , which in turn depends on the core frequency, ambient temperature, and the temperature of adjacent cores. The *fps* of a video is a performance metric that depends on the processor frequency.

Online RL. The primary objective in online reinforcement learning is to interact with an unknown Markov Decision Process (MDP), over a finite or infinite decision-making horizon \mathcal{H} , in order to optimize the policy π by observing transition trajectories τ_{MDP} . These trajectories are defined as $\tau_{\text{MDP}} = \{(s_0, a_0, r_1, s_1), (s_1, a_1, r_2, s_2), \dots, (s_{\mathcal{H}-1}, a_{\mathcal{H}-1}, r_{\mathcal{H}}, s_{\mathcal{H}})\}$. The transition trajectory is generated through the MDP setup, which consists of a continuous state space $\mathcal{S} \subseteq \mathbb{R}^d$ in a d -dimensional space, an action space $\mathcal{A} = \{a^{(0)}, a^{(1)}, \dots, a^{(k)}\}$ of k discrete actions, a state transition model with transition probability $P(s_{t+1} | s_t, a_t)$, a reward function $\mathcal{R}(\mathcal{S}, \mathcal{A})$, and a discount factor γ to account for the value of rewards over time. At each time step t , the system observes the previous and current states $s_t, s_{t+1} \in \mathcal{S}$, the current action $a_{t+1} \in \mathcal{A}$, and the current reward $r_{t+1} = \mathcal{R}(s_{t+1}, s_t, a_t)$. The objective of the MDP is to maximize the cumulative rewards, as expressed in Equation 1, where the optimal policy π^* determines the best action the agent can take to maximize this reward.

$$\text{Maximize } \sum_{t=1}^{\mathcal{H}} \gamma^t \mathcal{R}(s_{t+1}, s_t, a_t) \quad (1)$$

The policy π can be either deterministic, $\pi(s_t)$, where the action is chosen without randomness, or probabilistic, $\pi(a_t | s_t)$, where the action is chosen based on a probability distribution conditioned on the state s_t .

Multi-Armed Bandit Problem. The bandit problem is a simplified version of online reinforcement learning, where there is only one state s_t with a decision horizon of $H = 1$. The reward for taking action a_t at time t is given by $R(a_t) = r_t$. The resulting trajectory for the bandit problem can be represented $\tau_{\text{bandit}} = \{(a_0, r_0), (a_1, r_1), \dots, (a_T, r_T)\}$ as T stands for the total time steps. The regret Reg in this simplified scenario is defined as the difference between the expected reward of the best possible action and the expected reward obtained by the actions actually taken over time. This is expressed in Equation 2, where $\mu_r^* = \max_{a_t \in \mathcal{A}} \mathbb{E}[R(a_t)]$ represents the maximum expected reward based on the optimal action at each time step.

$$\text{Reg} = T \cdot \mu_r^* - \sum_{t=1}^T \mathbb{E}[R(a_t)] \quad (2)$$

Q-learning. The Q-function, denoted as $\mathcal{Q}(s_t, a_t)$, represents the expected cumulative reward for taking action a_t in state s_t and following the optimal policy thereafter. In continuous state spaces ($\mathcal{S} \subseteq \mathbb{R}^d$), Deep Q-Networks (DQNs) approximate the Q-function using weight parameters \mathcal{W} to capture the non-linear characteristics of the input features. The Q-function is updated based on observed trajectories using the following rule: $\mathcal{Q}(s_t, a_t; \mathcal{W}) \leftarrow \mathcal{Q}(s_t, a_t; \mathcal{W}) + \alpha [r_t + \gamma \max_{a'} \mathcal{Q}(s_{t+1}, a'; \mathcal{W}^-) - \mathcal{Q}(s_t, a_t; \mathcal{W})]$, where the immediate reward r_t and the discounted maximum future Q-value $\gamma \max_{a'} \mathcal{Q}(s_{t+1}, a'; \mathcal{W}^-)$ derived from a target network with older weights \mathcal{W}^- drive the update. The policy $\pi(a | s)$ is derived from the Q-function. In probabilistic ϵ -greedy algorithms, the policy selects a random action (*exploration*) with probability ϵ and the action that maximizes the Q-value (*exploitation*) with probability $1 - \epsilon$. In an ϵ -decay scenario, ϵ decreases over time, gradually shifting focus from exploration to exploitation as learning progresses.

Law of Large Numbers in Online RL. In online reinforcement learning, as the number of samples or total observed trajectories N increases, the empirical estimates of key quantities, such as the Q-function and transition probabilities, converge to their true expected values (denoted with an asterisk), as shown in Equation 3.

$$\begin{aligned} \lim_{N \rightarrow \infty} \mathcal{Q}_N(s, a; \mathcal{W}) &= \mathcal{Q}^*(s, a) \\ \lim_{N \rightarrow \infty} P_N(s_{t+1} | s_t, a_t) &= P^*(s_{t+1} | s_t, a_t) \end{aligned} \quad (3)$$

Flow Matching. Flow matching involves transforming a simple known distribution, typically Gaussian noise with mean 0 and standard deviation 1, denoted as $q_0(x) = \mathcal{N}(x | 0, 1)$, into a complex target distribution $q_1(x)$ along a probability density path $p_t(x)$. The generative process transitions from noise at $t = 0$ to data at $t = 1$. This transformation is governed by a time-dependent flow defined by a vector field $v(x(t))$ over the interval $[0, 1]$, which satisfies the ordinary differential equation (ODE):

$$\frac{dx(t)}{dt} = v(x(t)).$$

Given the probability density path $p_t(x)$ and a true vector field $w(x(t))$, the objective is to find a model $v_{\mathcal{W}}(x(t))$ with trainable parameters \mathcal{W} that minimizes the difference between the model and the true vector field. This is formulated as the following optimization problem:

$$\min_{\mathcal{W}} \mathbb{E}_{\substack{t \in [0, 1] \\ x_t \sim p_t(x)}} [\|v_{\mathcal{W}}(x(t)) - w(x(t))\|^2]. \quad (4)$$

However, directly optimizing Equation 4 is challenging because the true vector field $w(x(t))$ is unknown. To address this, we introduce a conditioning variable z that allows us to model the conditional probability density $p_t(x | z)$ and the corresponding conditional vector field $v(x(t); z)$. This leads to the following conditional flow matching objective, which is more tractable and has been shown to produce gradients similar to those in unconditional flow matching, as demonstrated in Lipman et al. [2022]:

$$\begin{aligned} \frac{dx(t)}{dt} &= v(x(t); z), \\ \min_{\mathcal{W}} \mathbb{E}_{\substack{t \in [0, 1] \\ x_t \sim p_t(x) \\ z \sim q(z)}} [\|v_{\mathcal{W}}(x(t); z) - w(x(t); z)\|^2]. \end{aligned} \quad (5)$$

As demonstrated in Lipman et al. [2022], incorporating conditional paths into the flow matching process does not alter the gradient structure. Moreover, compared to diffusion models, flow matching enhances both training efficiency and sample efficiency, resulting in improved model performance.

3 Design Of Distribution-Aware Flow Matching for Data Generation

The primary objective of this paper is to leverage flow matching due to its robustness and sample efficiency in generating synthetic data that closely resembles the extracted trajectories from the processor monitoring in real-world environments. The purpose of this synthetic data is to satisfy the LLN, as shown in Equation 3. While flow matching, with its ability to model the flow of density over time, is well-suited to structured data such as images and videos due to their inherent spatial correlations, unstructured data like features extracted from multi-core processors pose a different challenge. For instance, it is unclear how frames per second might change with variations in power consumption or how temperature might be affected by changes in frame rates. Additionally, collecting data for DVFS applications is time-consuming and may not capture all edge cases, such as determining the appropriate frequency when the processor is overheated. To address these challenges, we introduce a robust latent space through bootstrapping and preserve the correlation among features by weighting them appropriately in the flow estimation process.

To enhance the robustness and diversity of flow matching, we modify the latent space by incorporating bootstrapping into the sampling process Efron [1992]. Let $x(0) \sim p_0(x)$ represent the base distribution in the latent space. The bootstrapped sampling can be defined as $x(0)^b = \text{Resample}(x_0)$. We can generate multiple bootstrapped samples, denoted by $\{x(0)^b\}_{b=1}^B$, where B is the number of bootstrap samples. Consequently, $x(1)^b$ represents the generated sample from the bootstrapped latent sample $x(0)^b$. With bootstrapping, the unconditional objective function transforms from Equation 4 to Equation 6, and a similar transformation applies to the conditional flow matching objective in Equation 5. Here, $p_t^b(x)$ is the distribution of the bootstrapped latent representation at time t , and $x^b(t)$ denotes the latent representation generated at time t .

$$\min_{\mathcal{W}} \frac{1}{B} \sum_{b=1}^B \mathbb{E}_{\substack{t \in [0,1] \\ x_t \sim p_t^b(x)}} [\|v_{\mathcal{W}}(x^b(t)) - w(x^b(t))\|^2]. \quad (6)$$

By incorporating statistical bootstrapping of the latent representation, the model is exposed to a broader range of latent variations, which enhances its ability to generalize when generating new data. Additionally, bootstrapping increases the diversity of the latent space, making it particularly useful for scenarios where the target distribution is complex and highly variable. However, while this approach improves generalization and diversity, it does not inherently focus on the most critical aspects of the data during synthetic data generation.

To address this, we introduce feature weighting in the flow matching model as shown in Equation 6. This mechanism emphasizes the more critical features, helping to create structured patterns and maintain correlations among features in the synthetic data. Equation 7 presents the weighted version of the flow matching model from Equation 6, including the conditional flow matching. Here, λ_i represents the weight assigned to each feature, and the objective function sums over the weighted flow across all d features.

$$\min_{\mathcal{W}} \frac{1}{B} \sum_{b=1}^B \mathbb{E}_{\substack{t \in [0,1] \\ x_t \sim p_t^b(x) \\ z \sim q(z)}} \left[\sum_{i=1}^d \lambda_i \|v_{\mathcal{W}}(x_i^b(t); z) - w(x_i^b(t); z)\|^2 \right], \quad (7)$$

We incorporate a statistical feature selection method called Random Forest to weight the features. In this approach, the importance of each feature is evaluated based on its contribution to the transition function, specifically its ability to predict the current state given the previous state and action. These feature importances are then normalized as shown in Equation 8.

$$\lambda_i = \frac{\text{Importance}(x_i(t))}{\sum_{i=1}^d \text{Importance}(x_i(t))} \quad (8)$$

According to the LLN, if the synthetic data perfectly resembles the real data, the empirical estimates of the Q-function and the transition function will converge to their true expected values, as shown in Equation 3. Furthermore, assuming the total number of trajectories is N , the regret bound Reg for an ϵ -greedy algorithm decreases as N increases, indicating improved policy performance, as shown in Equation 9 Foster and Rakhlin [2023].

$$\text{Reg} \leq \mathcal{O} \left(\frac{1}{\sqrt{N}} \cdot T \cdot \sqrt{\log T} \right) \quad (9)$$

To increase the number of trajectories, we integrate synthetic data generated through distribution-aware flow matching instead of relying on environment modeling for data generation. In model-based RL, the environment's transition function $P(s_{t+1} | s_t, a_t)$ is modeled by predicting the future state s_{t+1} given the current state s_t and action a_t . This

Algorithm 1: Distribution Aware Flow Matching for Few-Shot Online RL.

```

1: Initialize: Replay memories  $\mathcal{M}$  and  $\mathcal{M}'$  for storing real-world and synthetic trajectory data with capacities  $|\mathcal{M}|$  and  $|\mathcal{M}'|$ ;
2: Initialize: Deep models  $DQN$  for agent and  $FM$  for environment model;
3: Set: exploit time  $\zeta_e$ , depth  $\zeta_d$ , breadth  $\zeta_b$ , and batch sizes  $\beta$ ;
4: Initialize memory counters  $\phi_{\mathcal{M}}, \phi_{\mathcal{M}'} = 0, 0$ ;
5: for  $i = 1$  to  $H$  do
6:   /* Direct Real-World Data Collection */
7:   Collect real-world trajectory  $\tau_{\text{real}}$ ;
8:   Store trajectory  $\tau_{\text{real}}$  in  $\mathcal{M}_{\text{real}}$ ;  $\phi_{\mathcal{M}} + +$ ;
9:   if  $i\% \zeta_d == 0$  and  $\phi_{\mathcal{M}} > \beta$  then
10:    Load all memory transitions  $\mathcal{M}$ ;
11:    Train model  $FM(\mathcal{M})$ ;
12:   end if
13:   /* Planning using Synthetic Data */
14:   for  $j = 1$  to  $\zeta_b$  do
15:    Generate synthetic trajectory  $\tau_{\text{synth}}$  using model  $FM$ ;
16:    Store synthetic trajectory  $\tau_{\text{synth}}$  in  $\mathcal{M}'$ ;  $\phi_{\mathcal{M}'} + +$ 
17:   end for
18:   if  $\phi_{\mathcal{M}} + \phi_{\mathcal{M}'} > \zeta_e$  then
19:    Sample transitions  $\tau_{\text{real}}$  and  $\tau_{\text{synth}}$ 
20:    Concatenate real-world and synthetic trajectory data;
21:    Train value functions  $DQN(\tau_{\text{real}} + \tau_{\text{model}})$ ;
22:   end if
23: end for

```

data generation step, known as *Planning*, is based on the trained model. However, a significant issue in model-based RL is that multiple predictions for the same action, with changes in state, can lead to highly correlated generated data, which may not accurately represent the real data. We address this problem by using distribution-aware flow matching, which trains on real trajectories and generates diverse samples, including different actions, states, next states, and rewards, for each synthetic trajectory.

The training architecture of DQN is inspired by Model-Based Dyna-Q architecture Peng et al. [2018], and is detailed in Algorithm 1. This method transitions from the traditional focus on state-action pairs to utilizing real-world trajectories as the basis for both training and planning. The approach involves two primary phases: **Direct Real-World Data Collection** and **Planning using Synthetic Data**.

In the first phase, replay memories \mathcal{M} and \mathcal{M}' are initialized to store real-world trajectory data and synthetic trajectory data, respectively. These memories are allocated specific capacities, denoted as $|\mathcal{M}|$ and $|\mathcal{M}'|$, to manage the data efficiently. The approach employs two deep models: the DQN model, which serves as the agent’s value function estimator, and the *Distribution-Aware Flow-Matching* (FM) model, which is responsible for generating synthetic trajectories by learning a transformation based on the real-world data.

During the **Direct Real-World Data Collection** phase, the agent interacts with the environment to collect real-world trajectories τ_{real} . These trajectories are stored in the replay memory \mathcal{M} , and the memory counter $\phi_{\mathcal{M}}$ is incremented with each new trajectory. Periodically, based on the accumulation of real-world data, the *Distribution-Aware Flow-Matching* model is trained to generate synthetic trajectories. These synthetic trajectories τ_{synth} are stored in the replay memory \mathcal{M}' .

In the *Planning* phase, the synthetic data generated by the Distribution-Aware Flow-Matching model is used to supplement the real-world data, allowing the **DQN** model to be trained on a combination of real and synthetic trajectories. This combination of data sources enhances the model’s ability to generalize and improves its overall performance.

4 Experiments

We developed a DQN agent based on the zTT framework Kim et al. [2021] to optimize system performance under specific thermal and power constraints. The experiments were conducted on the Jetson TX2, which features six CPU cores and an embedded GPU. We captured performance data, including *fps*, core frequencies (f), power consumption (ρ), and core temperatures (θ). The client collected state tuples $\{fps, f, \rho, \theta\}$, while the server, hosted in the cloud, assigned actions based on the available frequencies f . The workflow of the proposed method is illustrated in Figure 1. The experiment was designed to evaluate the agent’s ability to dynamically adjust the system’s frequency and power settings, ensuring optimal performance while maintaining system stability.

Key hyperparameters for this experiment included an action space of 12 possible actions, a target FPS of 60, and a target temperature of 50 degrees Celsius. The agent was trained using a discount factor of 0.99 and an initial learning

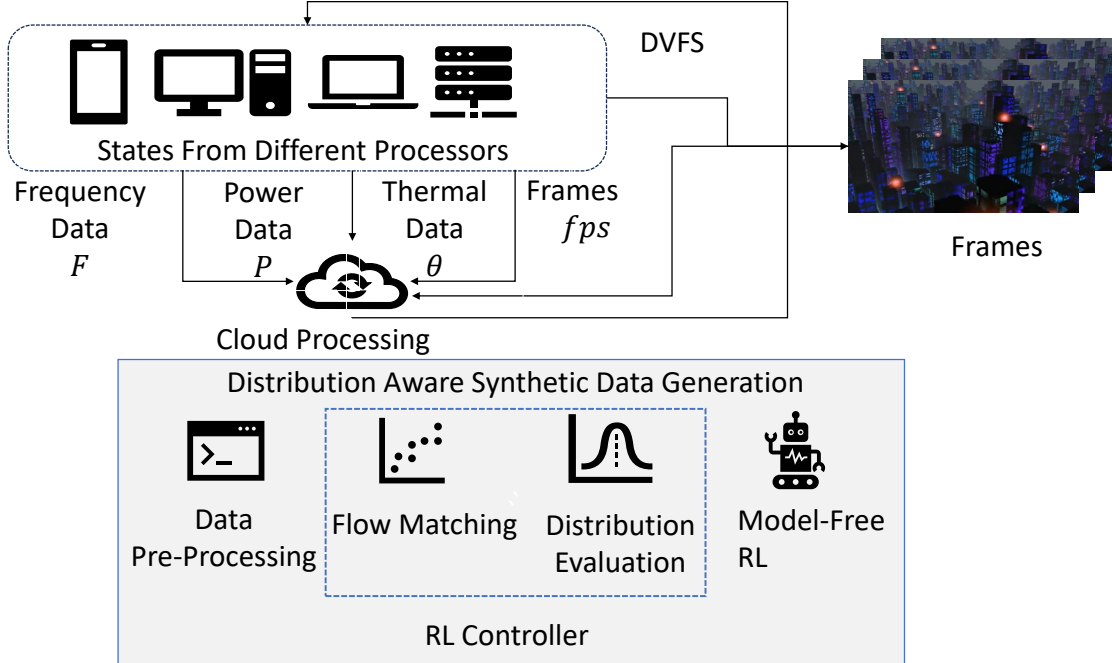


Figure 1: The workflow of the proposed distribution-aware flow matching RL.

rate of 0.05, which was dynamically adjusted during training. We conducted a grid search to tune the hyperparameters, and the selected values are highlighted in Table 1.

| Hyperparameter | Tuning Values |
|--------------------------|------------------------------------|
| Experiment Time | {50, 100, 200 , 400, 800} |
| Target FPS | {30, 60 , 90} |
| Target Temperature | { 50 , 60} |
| Learning Rate | {0.01, 0.05 } |
| Discount Factor | {0.95, 0.99 } |
| Epsilon Decay | {0.95, 0.99 } |
| Batch Size | { 32 , 64, 128} |
| Agent Train Start | { 32 , 40, 80, 100 } |
| Planning Iterations | {200, 1000 , 2000} |
| Model Train Start | { 32 , 200, 300} |
| Epochs | {200, 400 , 800} |
| Reward Scale (β) | { 2 , 4, 8} |

Table 1: Main Hyperparameters and Tuning Values for Grid Search

The DQN agent was implemented using a neural network with two hidden layers, each containing six neurons. The model was compiled with a mean squared error loss function and optimized using the Adam optimizer. The agent employed an epsilon-greedy policy for exploration, starting with an epsilon value of 1.0, which decayed over time to encourage exploitation of learned policies. The experiment was conducted over a set duration, with the agent making decisions at regular intervals. During each interval, the agent received state inputs—clock frequency, power consumption, temperature, and FPS—and selected an action to adjust the clock frequency. The environment responded by updating these state variables based on the selected action. The agent’s performance was evaluated based on the reward, calculated as a function of FPS, power consumption, and temperature.

We implemented a model-based RL to model the transition function, similar to the PlanGAN Algorithm developed in the Charlesworth and Montana [2020]. We employed a dual-memory strategy where real data was stored in one replay buffer, and synthetic data generated from a Flow Matching environment model was stored in another. The Flow Matching model, trained using the real data, allowed us to generate additional synthetic data, which the agent could use

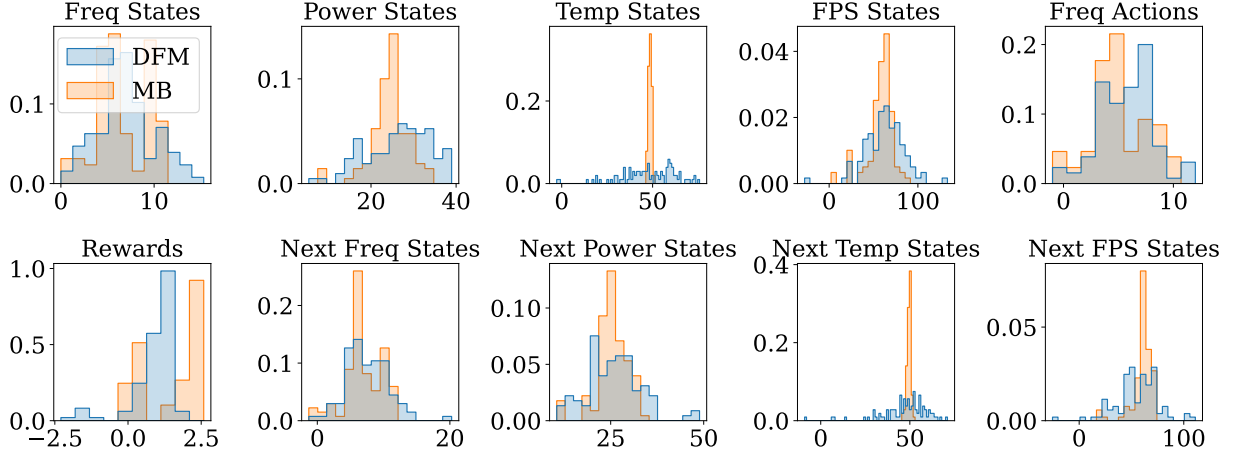


Figure 2: Comparing correlation matrix among states, actions, new states, reward, and done signal in four different methods.

for planning and further training. In model-based RL, after training a fully connected network (FCN), each planning iteration begins by sampling a random real-data point without replacement from the buffer to provide the simulation model with the initial state and action. The FCN then predicts the next state based on the number of planning iterations Peng et al. [2018].

In our developed flow matching method, we trained the conditional flow matching model from Tomczak [2022] using all the trajectories from real data stored in the buffer, then generated synthetic data based on this generative model. We then proceeded with distribution-aware flow matching and manipulation of the latent space, weighting the features, and regenerating the data.

We evaluated the correlation of synthetic features across three approaches and compared them with real data using Pearson’s correlation coefficient, as introduced in Sedgwick [2012]. This method determines the pairwise relationship between each pair of features, each with n samples, as shown in Equation 10. The resulting correlation coefficient corr_{ij} ranges between 1 and -1, where 1 indicates a positive correlation, -1 indicates a negative correlation, and 0 indicates no correlation between two features.

$$\text{corr}_{ij} = \frac{\sum_{k=1}^n (x_{i,k} - \bar{x}_i)(x_{j,k} - \bar{x}_j)}{\sqrt{\sum_{k=1}^n (x_{i,k} - \bar{x}_i)^2} \sqrt{\sum_{k=1}^n (x_{j,k} - \bar{x}_j)^2}} \quad (10)$$

The results in Figure 2 represents the correlation among the features in real-data, distribution-aware flow matching, pure flow matching, and model-based generated synthetic data. The Distribution-Aware method shows a correlation pattern that closely mirrors that of the real data, suggesting that it captures the underlying relationships between features more effectively than the other methods.

The Flow-Based method, while capturing some correlations, tends to dilute important relationships, as seen by the more uniform and less distinct correlation patterns compared to the Distribution-Aware method. This uniformity could lead to a less accurate model when applied to reinforcement learning tasks, as it might miss critical dependencies between features.

The Model-Based method, on the other hand, displays strong but often incorrect correlations, indicated by the intense colors in the wrong places. This suggests that the Model-Based approach might overfit to certain patterns, incorrectly estimating feature dependencies, which can be detrimental to the robustness of the learning process.

The Figure 3 illustrates the distribution of various states and actions generated by the Distribution-aware Flow Matching (DFM) and Model-Based (MB) approaches. In almost all cases, the Flow Matching method (depicted in blue) provides a broader and more diverse range of data, particularly in "Freq States," "Freq Actions," and "Rewards." This diversity is crucial for training robust reinforcement learning models, as it exposes the model to a wider variety of scenarios, potentially leading to more generalized and effective policies.

In contrast, the Model-Based approach (shown in orange) exhibits a more concentrated distribution, especially in "Power States," "Temp States," and "Next States" categories. Such narrow distributions may limit the model’s exposure

to diverse scenarios, risking overfitting and reduced generalization capability. This limitation could result in less robust policies when the model encounters situations outside its learned narrow distribution.

Overall, the Flow Matching method’s ability to generate more varied and distributed data makes it a superior approach for enhancing the diversity and robustness of synthetic datasets used in RL. This diverse data range can lead to better policy learning, improved generalization, and potentially higher performance in real-world applications.

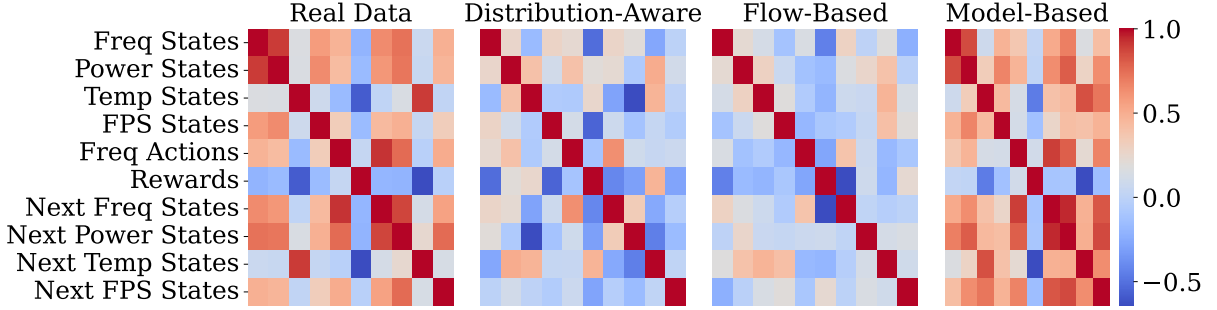


Figure 3: Comparing the distribution of the data in MB for modeling transition function and Distribution-Aware Flow Matching (DFM).

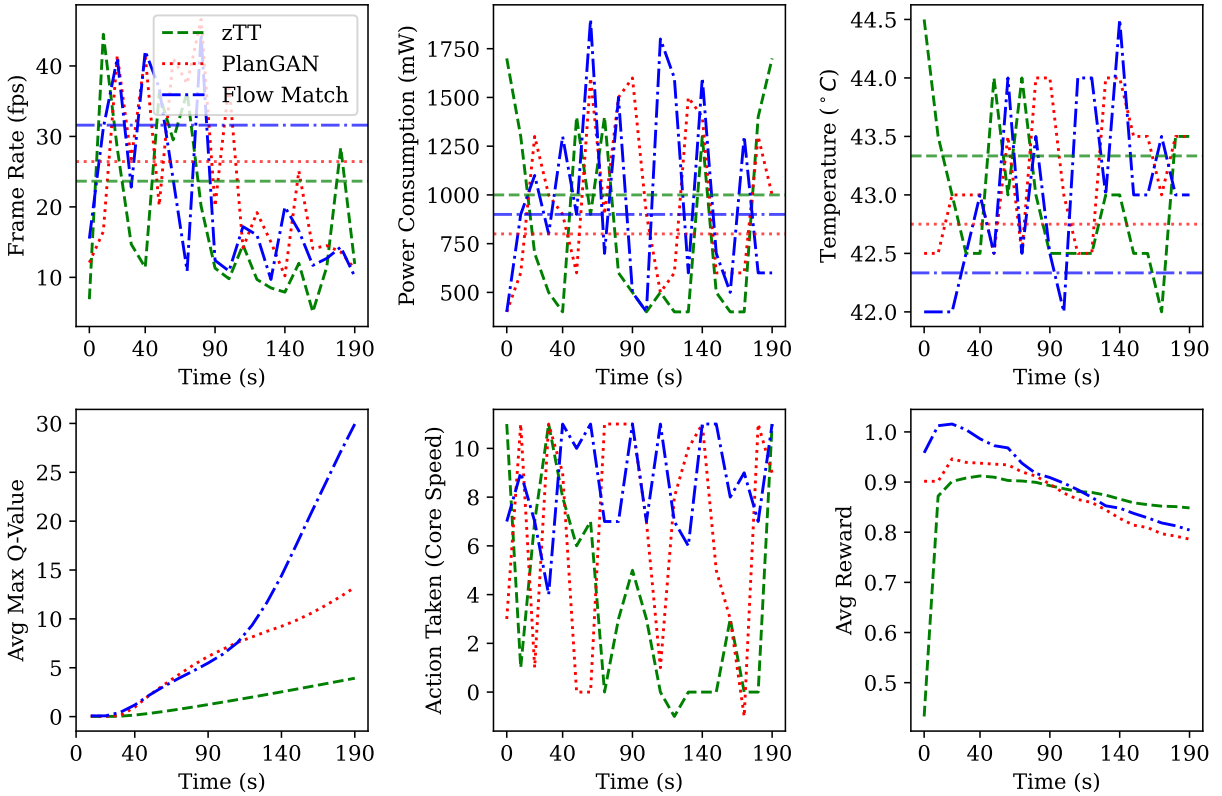


Figure 4: Comparing distribution-aware flow matching (DFM) with state of the art zTT and PlanGAN approach presented in Charlesworth and Montana [2020] and Kim et al. [2021] respectively.

This approach is based on a model-free framework in Kim et al. [2021] using a sample video with a 120 fps and a target of 60 fps in the reward definition. During the experiment, the agent’s performance metrics, including FPS, power consumption, average Q-values, and loss, were recorded and visualized in real-time. The agent’s decision-making process was guided by the rewards it received, which were influenced by the current system state and the difference

between the actual and target FPS and temperature. The learning rate of the agent was reset periodically to avoid overfitting and ensure that the model continued to generalize well to new data.

The experiment, as illustrated in Figure 4, demonstrated the efficacy of employing a Deep Q-Network (DQN) agent in conjunction with a synthetic data generation model (*DFM*) to optimize system performance under constrained conditions. The Frames Per Second (FPS) in the flow match algorithm, represented by the blue line, exhibit greater stability compared to the previous approach. The reward function, consistent with Kim et al. [2021], integrates FPS (fps), power consumption (ρ), and core temperatures (θ) as follows:

$$R = u + v + \frac{\beta}{\rho},$$

where

$$u = \begin{cases} 1 & \text{if } fps \geq \text{target_fps}, \\ \frac{fps}{\text{target_fps}} & \text{otherwise,} \end{cases}$$

and

$$v = \begin{cases} 0.2 \cdot \tanh(\text{target_temp} - \theta) & \text{if } \theta < \text{target_temp}, \\ -2 & \text{if } \theta \geq \text{target_temp}. \end{cases}$$

These constraints are dependent on the target FPS (here 60 FPS) and target temperature (here 50 °C), and the reward scale (β) which adjusts the importance of power efficiency in the reward value. According to the reward values depicted in Figure 4, the agent effectively balances the trade-offs between FPS, temperature, and power consumption, adapting swiftly to changing conditions by learning from both real and synthetic data.

DFM exhibits a more stable frame rate and manages power consumption effectively, characterized by fewer significant spikes and a controlled range. We observed an approximate **30% increase** in FPS within the first 50 timestamps compared to the model-free approach presented in Kim et al. [2021] when targeting a reward of 60 FPS. This improvement indicates superior handling of performance and power trade-offs, as well as enhanced policy learning facilitated by more reliable augmented data. In contrast, zTT exhibits greater fluctuations in both FPS and power consumption, suggesting inefficiencies in learning and policy application.

Additionally, DFM achieves higher average maximum Q-values more rapidly and maintains them with greater consistency, signifying faster and more reliable policy convergence. The steady average maximum Q-values indicate that the policy is stabilized to consistently select actions that maximize reward, unlike zTT and PlanGAN. This consistency in Q-values reflects a more robust learning process and effective policy enforcement, leading to sustained optimal performance across varying operational conditions.

5 Related Work

Machine Learning for DVFS. Due to the integration of DVFS technology in most commercial processors and their standard profiling and control, machine-learning algorithms are gaining importance in giving a global solution Yu et al. [2020], Kim and Wu [2020], Dinakarrao et al. [2019], Zhuo et al. [2021], Pagani et al. [2018], Shen et al. [2012], Wang et al. [2017], Yeganeh-Khaksar et al. [2020], Liu et al. [2021], Sethi [2021], ul Islam and Lin [2015], Wang et al. [2021], Bo et al. [2021]. The previous survey work Pagani et al. [2018] shows most of the machine learning algorithms for DVFS are based on model-free reinforcement learning, which implements a direct RL approach. None of the previous work address feature evaluation intricacies or sample collection overhead.

Statistical Learning for DVFS. Previous studies have examined statistical learning and the statistical significance of features based on hardware events and application parameters on DVFS performance Sasaki et al. [2007], Cazorla et al. [2019], Liu et al. [2021]. Sasaki et al. [2007] uses decision trees to reduce the overhead of table look-ups in low-energy DVFS. The authors in Cazorla et al. [2019] evaluate the importance of hardware counters in reducing energy consumption through DVFS. Liu et al. [2021] ranks compiler-generated feature correlation to latency using the f-scores. However, these studies ignore runtime performance metrics, sampling inefficiency, model accuracy, and their correlation evaluation for the learning model. Our distribution-aware DVFS provides a correlation evaluation and feature augmentation targeting low-energy high-performance DVFS.

Few Shot Learning. Few-shot learning on DVFS encompasses diverse methods such as transfer learning, meta-learning, model-learning, and data augmentation to reduce the data collection overhead Wang et al. [2020], Lee et al. [2020], Wang et al. [2016], Nachum et al. [2018], Florensa et al. [2017], Choi et al. [2017], Godbole et al. [2023], Chiley et al. [2019], Xu et al. [2015], Choi et al. [2017], Arora and Doshi [2021], Wulfmeier et al. [2015], Reddy et al. [2019], Vaswani et al. [2017]. Model-agnostic meta-learning adapts to new tasks with minimal data Finn et al. [2017], and model-based RL approximates transition functions to avoid the overhead of collecting real data Moerland et al. [2023], Charlesworth and Montana [2020]. Works in Lin et al. [2023], Kim et al. [2021], Zhou and Lin [2021], Zhang et al. [2024] utilize multi-agent RL, meta-state, transfer learning, and temporal dependencies on DVFS. None of these works address statistical resampling approaches for data augmentation or discovering the importance of energy consumption predictors for better task-to-core allocation.

6 Conclusion

This paper presented a distribution-aware flow matching approach to generate realistic and diverse unstructured data for few-shot RL, specifically applied to DVFS. By leveraging the sample efficiency of flow matching, combined with bootstrapping and feature weighting through Random Forests, our method addresses challenges like overfitting and data correlation in Model-Based RL. The approach aligns with the LLN, ensuring convergence to true empirical values and optimal policy decisions as sample size increases. Extensive experiments on low-energy processing demonstrated significant performance improvements in RL models operating in dynamic, resource-constrained environments. This framework enhances the adaptability and efficiency of RL models, providing a robust solution for real-time applications where data is limited. Our code is available upon request, supporting further research in this field.

References

- Aditya Ramesh, Prafulla Dhariwal, Alex Nichol, Casey Chu, and Mark Chen. Hierarchical text-conditional image generation with clip latents. *arXiv preprint arXiv:2204.06125*, 1(2):3, 2022.
- Chitwan Saharia, William Chan, Saurabh Saxena, Lala Li, Jay Whang, Emily L Denton, Kamyar Ghasemipour, Raphael Gontijo Lopes, Burcu Karagol Ayan, Tim Salimans, et al. Photorealistic text-to-image diffusion models with deep language understanding. *Advances in neural information processing systems*, 35:36479–36494, 2022.
- Florinel-Alin Croitoru, Vlad Hondru, Radu Tudor Ionescu, and Mubarak Shah. Diffusion models in vision: A survey. *IEEE Transactions on Pattern Analysis and Machine Intelligence*, 45(9):10850–10869, 2023.
- Yaron Lipman, Ricky TQ Chen, Heli Ben-Hamu, Maximilian Nickel, and Matt Le. Flow matching for generative modeling. *arXiv preprint arXiv:2210.02747*, 2022.
- Bradley Efron. Bootstrap methods: another look at the jackknife. In *Breakthroughs in statistics: Methodology and distribution*, pages 569–593. Springer, 1992.
- Trevor Hastie, Robert Tibshirani, Jerome H Friedman, and Jerome H Friedman. *The elements of statistical learning: data mining, inference, and prediction*, volume 2. Springer, 2009.
- Dylan J Foster and Alexander Rakhlin. Foundations of reinforcement learning and interactive decision making. *arXiv preprint arXiv:2312.16730*, 2023.
- Ivan Ratković, Nikola Bežanić, Osman S Ünsal, Adrian Cristal, and Veljko Milutinović. An overview of architecture-level power-and energy-efficient design techniques. *Advances in Computers*, 98:1–57, 2015.
- Guoqi Xie, Gang Zeng, Xiongren Xiao, Renfa Li, and Keqin Li. Energy-efficient scheduling algorithms for real-time parallel applications on heterogeneous distributed embedded systems. *IEEE Transactions on Parallel and Distributed Systems*, 28(12):3426–3442, 2017.
- Baolin Peng, Xiujun Li, Jianfeng Gao, Jingjing Liu, Kam-Fai Wong, and Shang-Yu Su. Deep dyna-q: Integrating planning for task-completion dialogue policy learning. *arXiv preprint arXiv:1801.06176*, 2018.
- Seyeon Kim, Kyungmin Bin, Sangtae Ha, Kyunghan Lee, and Song Chong. ztt: Learning-based dvfs with zero thermal throttling for mobile devices. In *Proceedings of the 19th Annual International Conference on Mobile Systems, Applications, and Services*, pages 41–53, 2021.
- Henry Charlesworth and Giovanni Montana. Plangan: Model-based planning with sparse rewards and multiple goals. *Advances in Neural Information Processing Systems*, 33:8532–8542, 2020.
- Jakub M Tomczak. *Deep Generative Modeling*. Springer Nature, 2022.
- Philip Sedgwick. Pearson’s correlation coefficient. *Bmj*, 345, 2012.

- Zheqi Yu, Pedro Machado, Adnan Zahid, Amir M Abdulghani, Kia Dashtipour, Hadi Heidari, Muhammad A Imran, and Qammer H Abbasi. Energy and performance trade-off optimization in heterogeneous computing via reinforcement learning. *Electronics*, 9(11):1812, 2020.
- Young Geun Kim and Carole-Jean Wu. Autoscale: Energy efficiency optimization for stochastic edge inference using reinforcement learning. In *2020 53rd Annual IEEE/ACM international symposium on microarchitecture (MICRO)*, pages 1082–1096. IEEE, 2020.
- Sai Manoj Pudukotai Dinakarrao, Arun Joseph, Anand Haridass, Muhammad Shafique, Jörg Henkel, and Houman Homayoun. Application and thermal-reliability-aware reinforcement learning based multi-core power management. *ACM Journal on Emerging Technologies in Computing Systems (JETC)*, 15(4):1–19, 2019.
- Cheng Zhuo, Di Gao, Yuan Cao, Tianhao Shen, Li Zhang, Jinfang Zhou, and Xunzhao Yin. A dvfs design and simulation framework using machine learning models. *IEEE Design & Test*, 2021.
- Santiago Pagani, PD Sai Manoj, Axel Jantsch, and Jörg Henkel. Machine learning for power, energy, and thermal management on multicore processors: A survey. *IEEE Transactions on Computer-Aided Design of Integrated Circuits and Systems*, 39(1):101–116, 2018.
- Hao Shen, Jun Lu, and Qinru Qiu. Learning based dvfs for simultaneous temperature, performance and energy management. In *Thirteenth International Symposium on Quality Electronic Design (ISQED)*, pages 747–754. IEEE, 2012.
- Zhe Wang, Zhongyuan Tian, Jiang Xu, Rafael KV Maeda, Haoran Li, Peng Yang, Zhehui Wang, Luan HK Duong, Zhifei Wang, and Xuanqi Chen. Modular reinforcement learning for self-adaptive energy efficiency optimization in multicore system. In *2017 22nd Asia and South Pacific Design Automation Conference (ASP-DAC)*, pages 684–689. IEEE, 2017.
- Amir Yeganeh-Khaksar, Mohsen Ansari, Sepideh Safari, Sina Yari-Karin, and Alireza Ejlali. Ring-dvfs: Reliability-aware reinforcement learning-based dvfs for real-time embedded systems. *IEEE Embedded Systems Letters*, 13(3): 146–149, 2020.
- Di Liu, Shi-Gui Yang, Zhenli He, Mingxiong Zhao, and Weichen Liu. Cartad: Compiler-assisted reinforcement learning for thermal-aware task scheduling and dvfs on multicores. *IEEE Transactions on Computer-Aided Design of Integrated Circuits and Systems*, 2021.
- Udhav Sethi. Learning energy-aware transaction scheduling in database systems. Master’s thesis, University of Waterloo, 2021.
- Fakhruddin Muhammad Mahbub ul Islam and Man Lin. Hybrid dvfs scheduling for real-time systems based on reinforcement learning. *IEEE Systems Journal*, 11(2):931–940, 2015.
- Yiming Wang, Weizhe Zhang, Meng Hao, and Zheng Wang. Online power management for multi-cores: A reinforcement learning based approach. *IEEE Transactions on Parallel and Distributed Systems*, 33(4):751–764, 2021.
- Zitong Bo, Ying Qiao, Chang Leng, Hongan Wang, Chaoping Guo, and Shaohui Zhang. Developing real-time scheduling policy by deep reinforcement learning. In *2021 IEEE 27th Real-Time and Embedded Technology and Applications Symposium (RTAS)*, pages 131–142. IEEE, 2021.
- Hiroshi Sasaki, Yoshimichi Ikeda, Masaaki Kondo, and Hiroshi Nakamura. An intra-task dvfs technique based on statistical analysis of hardware events. In *Proceedings of the 4th international conference on Computing frontiers*, pages 123–130, 2007.
- Francisco J Cazorla, Leonidas Kosmidis, Enrico Mezzetti, Carles Hernandez, Jaume Abella, and Tullio Vardanega. Probabilistic worst-case timing analysis: Taxonomy and comprehensive survey. *ACM Computing Surveys (CSUR)*, 52(1):1–35, 2019.
- Yaqing Wang, Quanming Yao, James T Kwok, and Lionel M Ni. Generalizing from a few examples: A survey on few-shot learning. *ACM computing surveys (csur)*, 53(3):1–34, 2020.
- Donghwan Lee, Niao He, Parameswaran Kamalaruban, and Volkan Cevher. Optimization for reinforcement learning: From a single agent to cooperative agents. *IEEE Signal Processing Magazine*, 37(3):123–135, 2020.
- Ziyu Wang, Tom Schaul, Matteo Hessel, Hado Hasselt, Marc Lanctot, and Nando Freitas. Dueling network architectures for deep reinforcement learning. In *International conference on machine learning*, pages 1995–2003. PMLR, 2016.
- Ofir Nachum, Shixiang Shane Gu, Honglak Lee, and Sergey Levine. Data-efficient hierarchical reinforcement learning. *Advances in neural information processing systems*, 31, 2018.
- Carlos Florensa, Yan Duan, and Pieter Abbeel. Stochastic neural networks for hierarchical reinforcement learning. *arXiv preprint arXiv:1704.03012*, 2017.

- Jinyoung Choi, Beom-Jin Lee, and Byoung-Tak Zhang. Multi-focus attention network for efficient deep reinforcement learning. *arXiv preprint arXiv:1712.04603*, 2017.
- Varun Godbole, George E. Dahl, Justin Gilmer, Christopher J. Shallue, and Zachary Nado. Deep learning tuning playbook, 2023. URL http://github.com/google/tuning_playbook. Version 1.0.
- Vitaliy Chiley, Ilya Sharapov, Atli Kosson, Urs Koster, Ryan Reece, Sofia Samaniego de la Fuente, Vishal Subbiah, and Michael James. Online normalization for training neural networks. *Advances in Neural Information Processing Systems*, 32, 2019.
- Kelvin Xu, Jimmy Ba, Ryan Kiros, Kyunghyun Cho, Aaron Courville, Ruslan Salakhudinov, Rich Zemel, and Yoshua Bengio. Show, attend and tell: Neural image caption generation with visual attention. In *International conference on machine learning*, pages 2048–2057. PMLR, 2015.
- Saurabh Arora and Prashant Doshi. A survey of inverse reinforcement learning: Challenges, methods and progress. *Artificial Intelligence*, 297:103500, 2021.
- Markus Wulfmeier, Peter Ondruska, and Ingmar Posner. Deep inverse reinforcement learning. *CoRR*, abs/1507.04888, 2015.
- Siddharth Reddy, Anca D Dragan, and Sergey Levine. Sqil: Imitation learning via reinforcement learning with sparse rewards. *arXiv preprint arXiv:1905.11108*, 2019.
- Ashish Vaswani, Noam Shazeer, Niki Parmar, Jakob Uszkoreit, Llion Jones, Aidan N Gomez, Łukasz Kaiser, and Illia Polosukhin. Attention is all you need. *Advances in neural information processing systems*, 30, 2017.
- Chelsea Finn, Pieter Abbeel, and Sergey Levine. Model-agnostic meta-learning for fast adaptation of deep networks. In *International conference on machine learning*, pages 1126–1135. PMLR, 2017.
- Thomas M Moerland, Joost Broekens, Aske Plaat, Catholijn M Jonker, et al. Model-based reinforcement learning: A survey. *Foundations and Trends® in Machine Learning*, 16(1):1–118, 2023.
- Chengdong Lin, Kun Wang, Zhenjiang Li, and Yu Pu. A workload-aware dvfs robust to concurrent tasks for mobile devices. In *Proceedings of the 29th Annual International Conference on Mobile Computing and Networking*, pages 1–16, 2023.
- Ti Zhou and Man Lin. Deadline-aware deep-recurrent-q-network governor for smart energy saving. *IEEE Transactions on Network Science and Engineering*, 9(6):3886–3895, 2021.
- Ziyang Zhang, Yang Zhao, Huan Li, Changyao Lin, and Jie Liu. Dvfo: Learning-based dvfs for energy-efficient edge-cloud collaborative inference. *IEEE Transactions on Mobile Computing*, 2024.